Journal of Solid Mechanics Vol. 9, No. 3 (2017) pp. 632-649

An Efficient Strain Based Cylindrical Shell Finite Element

M. Bourezane *

Civil Engineering Department, University of Biskra, BP 145 RP, 07000 Biskra, Algeria

Received 28 June 2017; accepted 26 August 2017

ABSTRACT

The need for compatibility between degrees of freedom of various elements is a major problem encountered in practice during the modeling of complex structures; the problem is generally solved by an additional rotational degree of freedom [1-3]. This present paper investigates possible improvements to the performances of strain based cylindrical shell finite element [4] by introducing an additional rotational degree of freedom. The resulting element has 24 degrees of freedom, six essential external degrees of freedom at each of the four nodes and thus, avoiding the difficulties associated with internal degrees of freedom (the three translations and three rotations) and the displacement functions of the developed element satisfy the exact representation of the rigid body motion and constant strains (in so far as this allowed by compatibility equations). Numerical experiments analysis have been conducted to assess accuracy and reliability of the present element, this resulting element with the added degree of freedom is found to be numerically more efficient in practical problems than the corresponding Ashwell element [4].

Keywords: Strain approach; Cylindrical finite element; Displacement functions; Rigid body modes.

1 INTRODUCTION

THE conventional analytical approaches to solutions of shells start with determining the necessary governing equations of the structure. These equations are generally obtained by first determining the necessary equilibrium equations of infinitesimal shell element. The equilibrium equations are generally not sufficient to determine all the unknowns and thus, resort to the relationships between internal and external forces are required. Existing analytical solutions to thin shell structural problems are, however, restricted in scope, and in general do not apply to arbitrary shapes and types of loading, irregular stiffening and support conditions, cut-outs and other aspects of practical designs. In such cases, the designer must resort to approximate the solutions. The usual approach is to establish a simplified model of the real structure by introducing some assumptions and reducing the problem in order to obtain solution. Engineers have long appreciated that the analysis of skeletal structures can be carried out by first, considering the behaviour of each individual element independently, and then assembling the elements together. In such a way, that equilibrium of forces and compatibility of displacements are satisfied at each nodal point. An example of such process is the analysis of a continuous beam by the slope-deflection method. However, analysing a structure that is comprised of many members is very laborious and is related implicitly to the solution of large number of simultaneous equations. Consequently, efforts were concentrated on the developments of the analytical

*Corresponding author. Tel.: 00213790673258.
E-mail address: bourmess@yahoo.fr (M. Bourezane).

technique based on physical appreciation of the structural behaviour which would reduce the amount of the required work to complete the analysis and would not require the direct solution of the many simultaneous equations. In addition to skeletal structures, engineers are often concerned with the analysis of continuum structures such as slabs, shell structures, dam walls and deep beams where the structural surface is continuous, instead of being composed of a number of individual components. Such continuum requires more sophisticated numerical techniques such as the finite deference or the finite element methods of analysis which are widely used in engineering problems. In the finite difference method, the derivatives appearing in the differential equations governing equilibrium and compatibility of a structural system are written in terms of the finite values at all adjacent nodes. Some modifications have to be applied on these equations in order to satisfy the boundary equations of the problem. Therein lays one of the difficulties and disadvantages of the method compared with the finite element method. On the other hand, the finite element method has proven to be more versatile and a better technique. The most significant advantages are the easy application of practical boundary conditions and the adaptability of the method to the coupling of beams and stiffeners with the shell. Several shell finite elements have been developed which lead to an improvement of the accuracy of the results. However, this improvement is achieved at the expense of increased computational effort and storage [5-7]. Attempts to develop a finite element for general shell structures have generally followed two different courses. In the first approach, the shell is replaced by an assemblage of flat plate elements that are either triangular or quadrilateral in shape. This approach has been successfully employed for cylindrical geometry [8] and for general shell shapes [9-11]. However, the disadvantage of the first approach is that there is no coupling between membranes and bending within each element, and to achieve satisfactory results, a large number of elements must be used. The second approach aims to develop curved shell elements that can represent geometrically shell structures. Consequently, successful cylindrical shell elements have been developed [12-14]. At Cardiff University, investigations on the suitability of the available finite elements for curved structures showed that to obtain satisfactory converged results, the assumed displacement elements required curved structure to be divided into a large number of elements [15]. Meanwhile, a simple alternative based on strain has been used to the development of shape functions, for a variety of curved elements [16-27]. These elements that are based on assumed strains rather than displacements satisfy the requirement of strain rigid body modes of displacement and they are based on independent strains assumptions that are allowed by the compatibility equations. The reasons for seeking an element based on strain functions rather than displacement functions [4] are:

Firstly, if we want to minimize the contribution of the strain energy to the potential energy of an element, we should seek variations of strain which are as smooth as possible.

Secondly, the equations relating displacements and generalized strains are, for curved element, coupled in such a way that some strains are functions of more than one displacement. Thus, if we make the displacements (u, v and w) independent of one another, the strain will not be so. These two considerations suggested that in seeking an element having general application to circular arches and rings, we should consider simple, independent, strain functions rather than displacement functions, and the success of the resulting element encouraged us to apply the same method to develop a cylindrical shell element. The advantage in assuming strains rather than stresses is that corresponding displacement functions can be obtained by straightforward integration of the strain-displacement relationships, and consequently the usual finite element procedures for calculating the element stiffness matrix from the displacement functions can then be applied. The success of the strain application approach to shell problems in linear analysis prompted the extension of the work to a large deflection nonlinear analysis [28, 29].

In this paper, the strain approach is also employed to develop a new cylindrical finite element based on the (Kirchhoff- Love) theory for solving cylinder problems for a thin and thicker shell. This element is found numerically more efficient with the added degree of freedom than the corresponding element [4], and its precision is evaluated through a series of tests related to thin and thicker shells.

2 THEORETICAL CONSIDERATIONS AND DEVELOPMENT OF THE PRESENT ELEMENT

Consider a cylindrical shell element with curvilinear coordinate system shown in Fig. 1. The displacements in the x, y, and z directions are u, v, and w respectively. This element is rectangular in plane with four corner nodes, and considers also the following element data:

a: length of straight sides
b: length of curved sides
r: the radius of the unstrained mid surface
β : half angle subtended by element

ϕ : angular coordinate

t: shell thickness

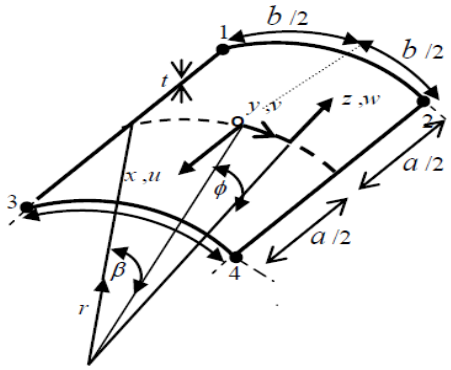

Fig.1
An element with coordinate $\phi = y / r$.

2.1 Strain-displacement equations used

The strain-displacement equations are taken from [30]; note that we have reversed the direction of the displacement w, they become:

$$\varepsilon_x = \frac{\partial u}{\partial x}, \varepsilon_\phi = \frac{\partial v}{r\partial \varphi} + \frac{w}{r}, \varepsilon_{x\phi} = \frac{\partial u}{r\partial \varphi} + \frac{\partial v}{\partial x}, \chi_x = -\frac{\partial^2 w}{\partial x^2}, \chi_\phi = \frac{1}{r^2}\left(\frac{\partial v}{\partial \phi} - \frac{\partial^2 w}{\partial \phi^2}\right), \chi_{x\phi} = \frac{1}{r}\left(-\frac{\partial^2 w}{r\partial x\,\partial \phi} + \frac{\partial v}{r\partial x}\right) \tag{1}$$

The above six strains given by (1) are used to obtain the three compatibility equations by eliminating *u, v* and *w* from them, hence

$$\frac{\partial^2 \varepsilon_\phi}{\partial x^2} + \frac{\chi_x}{r} + \frac{\partial^2 \varepsilon_x}{r^2 \partial \phi^2} - \frac{\partial^2 \varepsilon_{x\phi}}{r\partial x\,\partial \phi} = 0, \frac{\partial \chi_{x\phi}}{\partial x} - \frac{\partial \chi_x}{r\partial \phi} + \frac{\partial \varepsilon_x}{r^2 \partial \phi} - \frac{\partial \varepsilon_{x\phi}}{r\partial x} = 0, \frac{\partial \chi_x}{\partial x} - \frac{\partial \chi_{x\phi}}{r\partial \phi} = 0 \tag{2}$$

2.2 The degrees of freedom to be used

In order to keep the element shown in Fig. 1 as simple as possible, and to avoid the difficulties associated with internal and "non-geometric" degrees of freedom such as $u_x\,(=\partial u/\partial x)$ and $w_{x\phi}$, we choose six degrees of freedom at each node, namely $u, v, w, w_x, (w_\phi - v)/r, (v_x - u_y)/2$. Thus, the rectangular element has 24 degrees of freedom and 24×24 stiffness matrix. The displacement function of the element will contain 24 constants $\alpha_1, \alpha_2, ...\alpha_{24}$.

2.3 Derivation of the displacement function

Eq. (1) is integrated with all the strains equal to zero, thus obtaining

$$u_0 = r\alpha_2 \cos\phi + r\alpha_4 \sin\phi + \alpha_5 \tag{3a}$$

$$v_0 = (\alpha_1 + \alpha_2 x)\sin\phi - (\alpha_3 + \alpha_4 x)\cos\phi + \alpha_6 \tag{3b}$$

$$w_0 = -(\alpha_1 + \alpha_2 x)\cos\phi - (\alpha_3 + \alpha_4 x)\sin\phi \tag{3c}$$

$$\phi_{y0} = \frac{\partial w_0}{\partial x} \tag{3d}$$

$$\phi_{x0} = \frac{\partial w_0}{\partial \varphi} - \frac{v_0}{r} \tag{3e}$$

$$\phi_{z0} = \frac{\partial v_0}{2\partial x} - \frac{\partial u_0}{2r\partial \phi} \tag{3f}$$

Eq.(3) represents displacement function without strain corresponding to rigid body motion $\{\delta_0\}$: $\{\delta_0\} = \{u_0, v_0, w_0, \phi_{x0}, \phi_{y0}, \phi_{z0}\}^T$, its derivation is given in Appendix C [3].

The present element shown in Fig. 1 is rectangular in plane with four corner nodes, and each node has six degrees of freedom. Thus, the element displacement function should contain 24 independent constants. Six constants ($\alpha_1, \alpha_2, ...\alpha_6$) are used for the representation of the rigid body components. The remaining 18 are available for expressing the deformation of the element. These are apportioned among the six strains as:

$$\varepsilon_x = \alpha_7 + \alpha_8\phi + \alpha_{21}\phi^2 + 2\alpha_{22}x\,\phi^3 + [2r\alpha_{23}\phi] \tag{4a}$$

$$\varepsilon_\phi = \alpha_9 + \alpha_{10}x + [-\alpha_{12}x^2/2r - \alpha_{13}x^3/6r - \alpha_{14}x^2\phi/2r - \alpha_{15}x^3\phi/6r] - \alpha_{21}x^2 - 2\alpha_{22}x^3\phi \tag{4b}$$

$$\varepsilon_{x\phi} = \alpha_{11} + \alpha_8 x/r + 2\alpha_{23}x + 2\alpha_{24}\phi + [\left(2\alpha_{21}x\phi + 3\alpha_{22}x^2\phi\right)/r] \tag{4c}$$

$$\chi_x = \alpha_{12} + \alpha_{13}x + \alpha_{14}\phi + \alpha_{15}x\phi + [r\left(2\alpha_{21}x\phi + 3\alpha_{22}x^2\phi^2\right)] \tag{4d}$$

$$\chi_\phi = \alpha_{16} + \alpha_{17}x + \alpha_{18}\phi + \alpha_{19}x\phi \tag{4e}$$

$$\chi_{x\phi} = \alpha_{20} + \alpha_{14}x/r + \alpha_{15}x^2/2r + \alpha_{17}r\phi + \alpha_{19}r\phi^2/2 + [6\alpha_{22}x^2] \tag{4f}$$

In the above Eq. (4), the fourteen constants, $(\alpha_7 - \alpha_{20})$ were apportioned in the same way as [4] shown in Appendix A. The additional four constants $(\alpha_{21} - \alpha_{24})$ are then added to allow the in-plane rotations at the corners, the bracketed terms are added so that, the compatibility Eq. (2) is satisfied.

Expressions (4) are equated to the corresponding expressions in terms of *u, v* and *w* from Eq. (1) and the resulting equations integrated, to give displacement with strain $\{\delta_s\} = \{u_s, v_s, w_s, \phi_{ys}, \phi_{xs}, \phi_{zs}\}^T$ as:

$$u_s = \alpha_7 x + \alpha_8 x\phi + \alpha_{11}r\phi + \alpha_{17}r^3\phi^2/2 + \alpha_{19}\left(\left(r^3\phi - r^3\phi^3\right)/6\right) - \alpha_{20}r^2\phi + \alpha_{21}\phi^2 x + \alpha_{22}x^2\phi^3 + \alpha_{23}\left(2r\phi x\right) + \alpha_{24}r\phi^2 \tag{5a}$$

$$v_s = \alpha_{16}r^2\phi + \alpha_{17}r^2 x\phi + \alpha_{18}r^2\phi^2/2 + \alpha_{19}(-r^2 x + r^2 x\phi^2/2) + \alpha_{20}rx \tag{5b}$$

$$w_s = \alpha_9 r + \alpha_{10}rx - \alpha_{12}x^2/2 - \alpha_{14}x^2\phi/2 - \alpha_{15}\phi x^3/6 - \alpha_{16}r^2 - \alpha_{17}r^2 x - \alpha_{18}r^2\phi - \alpha_{19}r^2\phi x - \alpha_{20}x^3/2 - \alpha_{21}rx^2 + \alpha_{22}\left(2rx^3\phi\right) \tag{5c}$$

$$\phi_{ys} = \partial w/\partial x \tag{5d}$$

$$\phi_{xs} = (\partial w_s/\partial\phi - v_s)/r \tag{5e}$$

$$\phi_{zs} = (\partial v_s/\partial x - \partial u_s/r\partial\phi)/2 \tag{5f}$$

The total displacement function is the sum of corresponding expressions from Eqs. (3) and (5) $\{\delta\} = \{\delta_0\} + \{\delta_s\}$:

$$u = \alpha_2 r\cos\phi + \alpha_4 r\sin\phi + \alpha_5 + \alpha_7 x + \alpha_8 x\phi - \alpha_{11} r\phi + \alpha_{17} r^3\phi^2/2 - \alpha_{19}((r^3\phi - r^3\phi^3)/6) - \alpha_{20} r^2\phi + \alpha_{21}\phi^2 x + \alpha_{22} x^2\phi^3 + \alpha_{23} 2r\phi x + \alpha_{24} r\phi^2 \quad (6a)$$

$$v = (\alpha_1 + \alpha_1)\sin\phi - (\alpha_1 + \alpha_1)\cos\phi + \alpha_6 + \alpha_{16} r^2\phi + \alpha_{17} r^2\phi x + \alpha_{18}(r^2\phi^2/2) + \alpha_{19}(-r^2\phi x + r^2 x\phi^2/2 + \alpha_{20} rx \quad (6b)$$

$$w = -(\alpha_1 + \alpha_2 x)\cos\phi - (\alpha_2 + \alpha_4 x)\sin\phi + \alpha_9 r + \alpha_{10} rx - \alpha_{12} x^2/2 - \alpha_{14}(x^2\phi/2) + \alpha_{15}(-\phi x^3 x/6) - \alpha_{16} r^2 - \alpha_{17} r^2 x - \alpha_{18} r^2\phi - \alpha_{19} r^2\phi x - \alpha_{20} x^3/2 - \alpha_{21} rx - \alpha_{22} 2rx^3\phi \quad (6c)$$

$$\phi_y = \partial w/\partial x \quad (6d)$$

$$\phi_x = (\partial w/\partial\phi - v)/r \quad (6e)$$

$$\phi_z = (\partial v/\partial x - \partial u/r\partial\phi)/2 \quad (6f)$$

2.4 Derivation of the stiffness matrix [K^e]

By assuming the displacement function (6):

$$\{\delta(x,y)\} = [f(x,y)] \times \{\alpha\} \quad (7)$$

where

$\{\delta(x,y)\}$: represents the displacement vector at any point within the element.

$[f(x,y)]$: represents the polynomial function matrix.

$\{\alpha\}$: represents the constant terms vector.

By substituting the values of the nodal coordinates into Eq. (7), to give

$$\{\delta^e\} = [A] \times \{\alpha\} \quad (8)$$

where

$\{\delta^e\} = \{u_1, v_1, w_1, \phi_{y1}, \phi_{x1}, \phi_{z1}, ..., u_4, v_4, w_4, \phi_{y4}, \phi_{x4}, \phi_{z4}\}^T$

$\{\delta^e\}$: represents the nodal degrees of freedom of the element.

$\{\alpha\} = \{\alpha_1, \alpha_2, ..., \alpha_{24}\}$

The matrix [A] is presented in Appendix B.

Relating strains at any point in element to nodal displacements by considering Eqs. (1) and (8).

$$\{\varepsilon(x,y)\} = [B] \times [A]^{-1} \{\delta^e\} \quad (9)$$

where

$[B]$: represents the strain matrix which is given in Appendix B for the case of present element.

$\{\sigma\} = [D] \times \{\varepsilon\} = [D] \times [B] \times [A]^{-1} \times \{\delta^e\}$

$[D]$: represents rigidity matrix

where

$$[D]=\begin{bmatrix} D_1 & D_2 & 0 & 0 & 0 & 0 \\ D_2 & D_1 & 0 & 0 & 0 & 0 \\ 0 & 0 & D_3 & 0 & 0 & 0 \\ 0 & 0 & 0 & K_1 & K_2 & 0 \\ 0 & 0 & 0 & K_2 & K_1 & 0 \\ 0 & 0 & 0 & 0 & 0 & K_3 \end{bmatrix}$$

The rigidity matrix contains D_i and K_i terms, which are defined as:

$$D_1=\frac{Et}{1-\nu^2}, D_2=\nu D_1, D_3=\frac{1}{2}(1-\nu)D_1$$
$$K_1=\frac{Et^3}{12(1-\nu^2)}, K_2=\nu K_1, K_3=\frac{1}{2}(1-\nu)K_1$$

The total potential energy $\Pi = U - V$
U: The internal work done by the internal stresses (strain energy stored)
V: The external work done by the applied loads (the potential energy)

$$\begin{aligned} U &= \frac{1}{2}\int \{\varepsilon\}^T \{\sigma\} dvol \\ &= \frac{1}{2}\int \{\delta^e\}^T \times [A^{-1}]^T \times [B]^T \times [D] \times [B] \times [A]^{-1} \times \{\delta^e\} dvol \end{aligned} \tag{10}$$

$$V = \frac{1}{2} \times \{\delta\}^T \{p\} \tag{11}$$

By applying the principle of minimum potential energy:

$$\frac{\partial \pi}{\partial \{\delta^e\}} = \int [A^{-1}]^T \times [B]^T \times [D] \times [B] \times [A]^{-1} \times \{\delta^e\} dvol - \{p\} = 0 \tag{12}$$

$$\{p\} = [K^e] \times \{\delta^e\} \tag{13}$$

$$[K^e] = [A^{-1}]^T \left[\int [B]^T \times [D] \times [B] dvol \right] [A]^{-1} = [A^{-1}]^T \times [K_0] \times [A^{-1}] \tag{14}$$

Since the matrix $[A]$ of the present element is not singular, its inverse can be numerically evaluated and the element stiffness can be obtained. The matrix $[K_0]$ is analytically calculated by hand that is given in Appendix B.

3 PROBLEMS CONSIDERED

Performance of the developed cylindrical shell finite element is evaluated by working through four numerical examples, applications have been selected because they have analytical solutions and they are also standard problems for cylindrical shell analysis.

3.1 Pinched cylinder problem with free edges

The first problem to be considered is that of a pinched cylinder with free edges, as shown in Fig. 2, has been used as a test problem by many authors [4]. The numerical results for these elements are compared with the theoretical solution and the numerical results reported in the literature for the performance of other elements. Table 1. contains a summary of numerical results, with the asterisk (* or **) denoting the strain based element (*) or (**) displacement based element.

It would be interesting to have comparable results obtained by [4], [31] elements and present element described herein, as shown in Table 1.

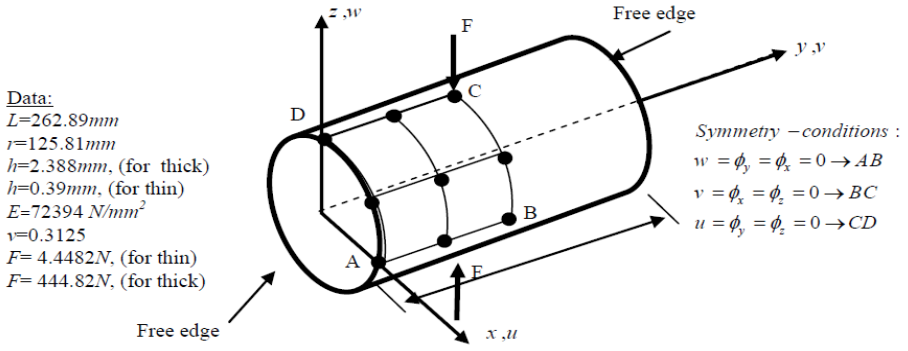

Fig.2
The pinched cylinder with one octant shown with free edges.

The present element gives acceptable results comparing with analytical solution, where the corresponding results are much better than those of [13] and [17]. A summary of results is provided in Fig. 3. Again, the present element generates displacements that are closer to the theoretical solution as predicted by the best shell element [4].

The results considered above are for a cylinder having $r/h = 53$ (where h is the thickness). It is interesting to note that single element on the present element with 24 degrees of freedom gives a closer result than a 2×2 mesh of [32] with 54 degrees of freedom. We conclude from Table 2. that the present element converges slightly faster than [32] element.

Table 1
Comparison of present element with other elements deflection w_c (mm) under one load for thin pinched cylinder problem (h=0.3927 mm).

8Mesh	[31]* (20 DOF)	[4]* (20 DOF)	[13]** (24 DOF)	[17]** (20 DOF)	[PE]* (24 DOF)
1×1	—	0.5 9106	0.00025	0.00025	0.5 9106
1×4	—	0.6 1773	0.01880	0.16002	0.6 1773
1×8	—	0.6 1849	0.17780	0.17551	0.6 1722
2×1	—	0.5 9106	0.00025	0.00025	0.5 9106
2×4	—	0.6 1900	0.01778	0.01626	0.6 1798
2×8	—	0.6 2027	0.17755	0.17628	0.6 2027
3×1	—	0.5 9131	0.01727	0.00025	0.5 9131
3×4	—	0.6 2052	0.17755	0.01651	0.6 1798
3×8	—	0.6 2154	0.00025		0.6 2154
4×4	0.62154	0.62179	—	—	0.6 1849
6×6	0.62357	0.62332	—	—	0.6 2103
8×8	0.62484	0.62382	—	—	0.6 2179
Analytical –S(mm)			0.61951		

DOF: degree of freedom, *[PE]: present element with 24 degrees of freedom.

Table 2
Comparison of present element with other elements deflection w_c (*mm*) under one load for thick pinched cylinder problem (*h*=2.3876 *mm*).

Mesh	[4]*	[32]**	[31]*	[PE]*
1×1	2. 6416	-	2. 6416	2. 6441
2×2	2. 8067	2. 3647	2. 8042	2. 8092
4×4	2. 8778	2.8600	2. 8727	2. 8829
6×6	2. 8905	2. 8880	2. 8905	2. 8956
8×8	2. 9007	2. 8931	2. 8956	2. 9007
10×10	2. 8981	2. 8931	2. 8981	2. 8981
Reference(*mm*)		2. 8931		

*[PE]: present element with 24 degrees of freedom.

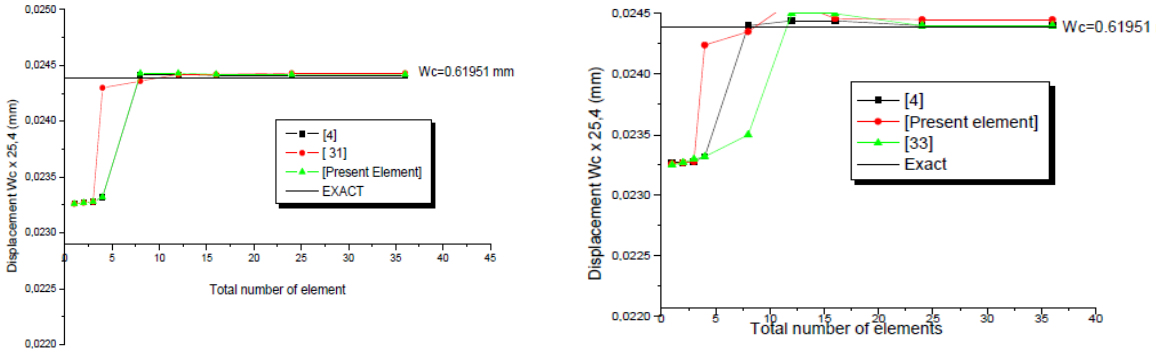

(a) (b)

Fig.3
Convergence of displacement w_c for thin pinched cylinder with free edges (*h*=0.39319*mm*).

Selected convergence curves for thick pinched cylinder problem with free edges (*h*=2.3876 *in*) show that the present element and that of [4] provide much greater accuracy than element of [33], and they are in good agreement with the theoretical solution, shown in Fig. 4.

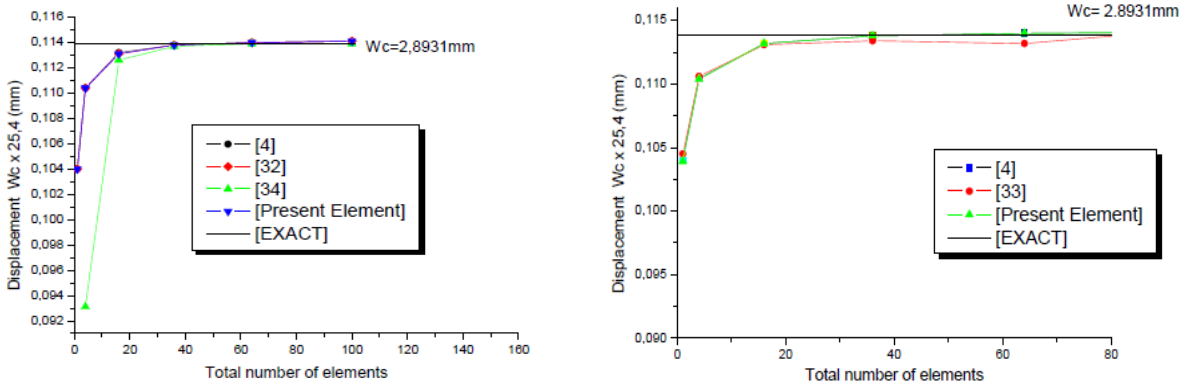

(a) (b)

Fig.4
Convergence of displacement w_c for thick pinched cylinder with free edges (*h*=2.876*mm*).

3.2 Pinched cylinder problems with diaphragm

The second problem to be considered is that of a pinched cylinder with diaphragms having the geometry as shown in Fig.5. It has been used as a test problem by many authors [34]. This test constitutes one of the most severe tests to

study the capacity of shell element to describe fields of complex membrane strains with a significant part of bending without extension of middle surface. An analytical solution was presented by [5].

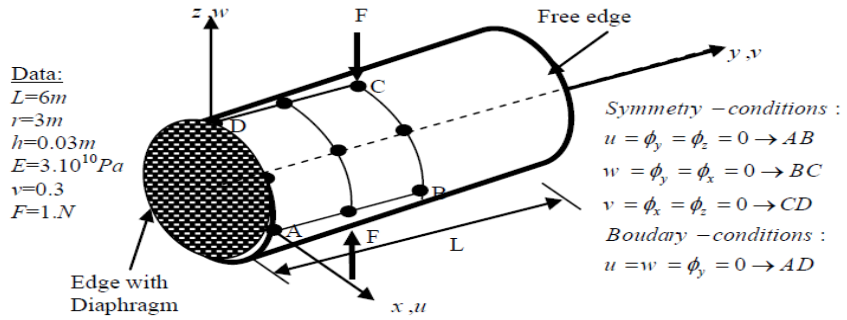

Fig.5
Pinched cylinder with rigid diaphragm, geometry, data and one octant shown.

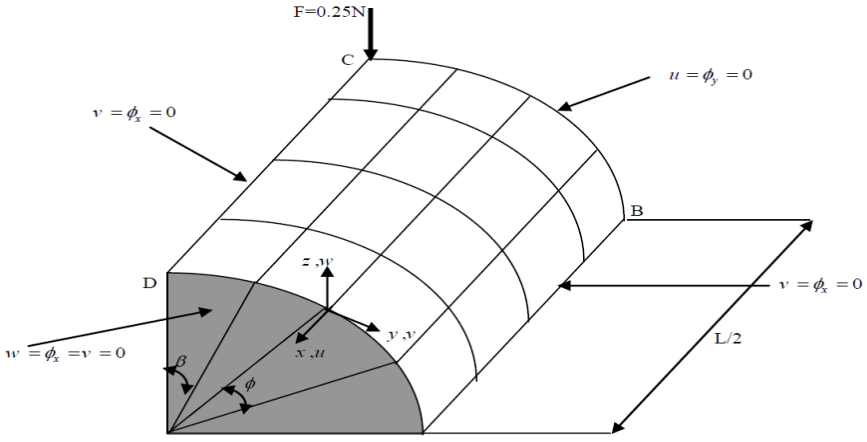

Fig.6
Meshes 4x4 of pinched cylinder with rigid diaphragm.

The numerical results for the present element are compared with the theoretical solution, and numerical results reported in the literature for the performance of other elements. Figs. 7 and 8 contain a summary of numerical results, these results lead to the following remarks:

A monotonous convergence of displacement for all the elements is observed.

Good results are obtained with present element for this problem.

With identical number of elements, [17] element gives better results than other elements.

The normal displacements (w_c) in both directions DC and BC, also tangential displacement (u_c), are shown in Fig. 9. From the Fig. 9, we can see that the displacement computed by present element and that of [34] are in very close agreement.

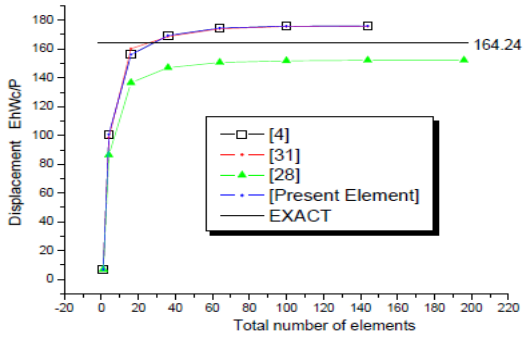

Fig.7
Convergence of displacement w_c for pinched cylinder with rigid diaphragm.

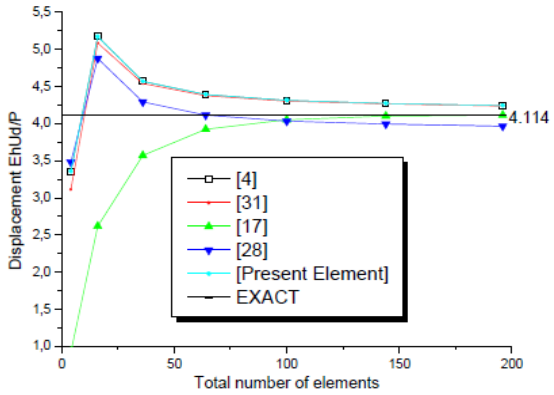

Fig.8
Convergence of displacement U_d for pinched cylinder with rigid diaphragm.

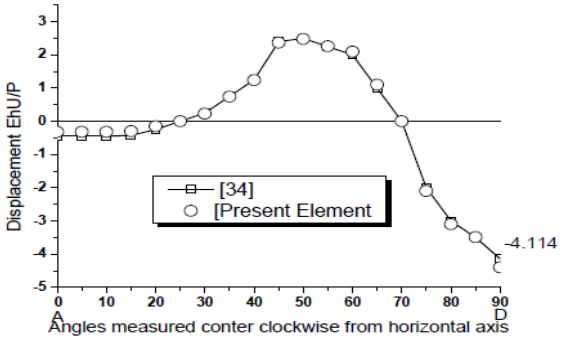

(a)

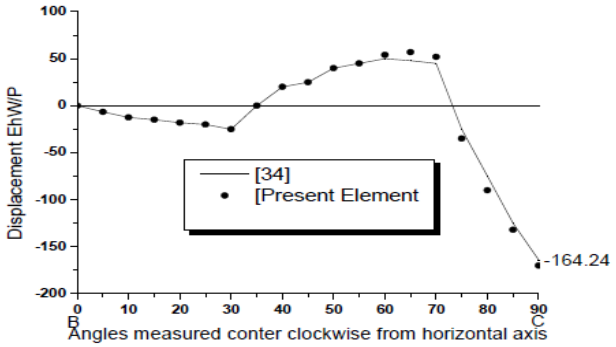

(b)

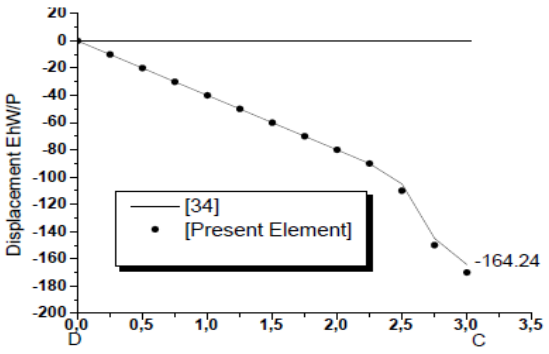

(c)

Fig.9
a) Displacement in *Z* direction, along AD for pinched cylinder problems with rigid diaphragm. b) Displacement in *Z* direction, along BC for pinched cylinder problems with rigid diaphragm (R/h=100). c) Displacement along DC(R/h=100) for pinched cylinder problems with rigid diaphragm.

3.3 Cylindrical panel subjected to its own weight (barrel vault problem)

Other authors have used a barrel vault problem as a test for finite elements. The straight edges are free and the curved edges are supported by diaphragms. Geometry, properties and loading are indicated in Fig.10: (r /h = 100, L/h = 200). The transverse shearing strains are negligible where, the membrane strains are important compared to those of bending. This problem is used as an aptitude test of an element to simulate membrane state of stresses (strains). The quarter of the roof is modelled by considering regular grids with N=4, 6 and 8 elements on edges AB and AD.

Fig.11 gives convergence data for a number of different elements, the present element gives a similar convergence curve to that of reference [4]. The present element, [17] and [4] converge towards the solution of deep shells. The effects of membrane are relatively important to [28] element converges towards the solution of shallow shells.

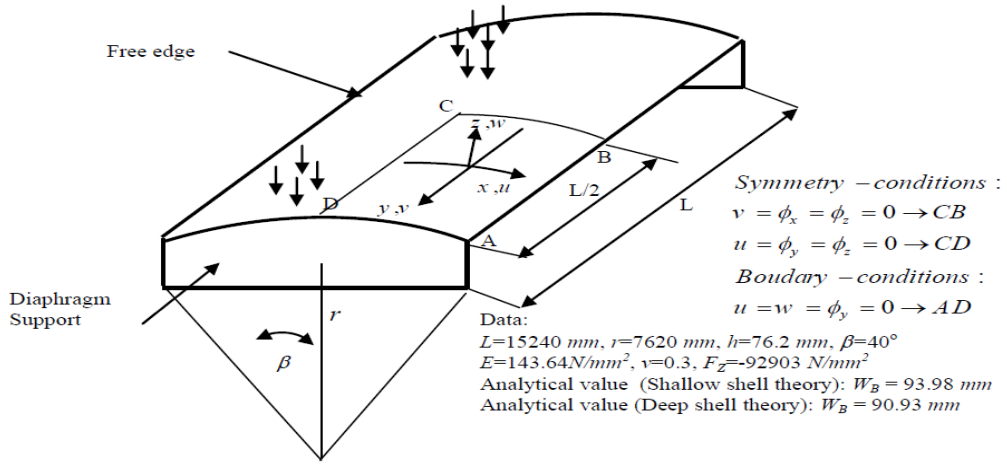

Fig.10
The barrel vault problem. The loading is a uniform gravity loading of 92903N/mm^2 of shell area.

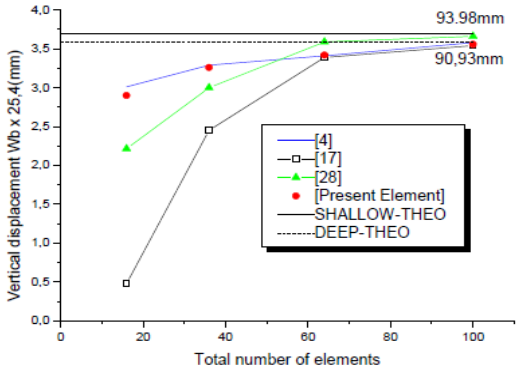

Fig.11
Convergence of vertical displacement WB. For barrel vault using total number of elements.

3.4 Curved cantilever beam

Geometry, properties and loading of curved cantilever beam are shown in Fig. 12. The beam is analyzed with the finite element idealizations given in Fig. 13 in different load cases (in plane and out of plane load cases) as suggested in [35]. The results given by beam theory and [4] are shown in Table 3. for the tip displacements which are in good agreement with those of present element. The variation of the tip displacements versus the total number of element is shown in Fig. 14 which shows that the results obtained using the present element are compared well with those given by other elements [17], [33] and [4].

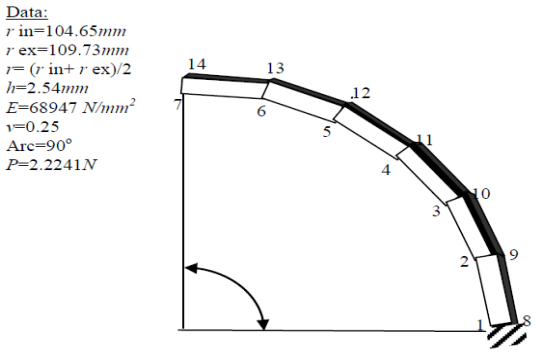

Fig.12
Shell-Curved Beam.

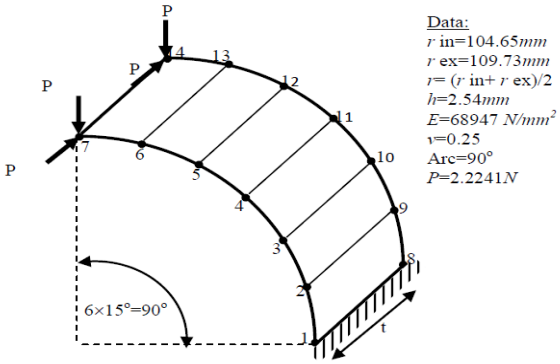

Fig.13
Shell-Curved Beam with Static Loads.

Table 3
Results of deflection (mm) in the load direction for Curved Beam under Static Loads.

Mesh	Load case			
	In-plane		Out-of-plane	
	[4]	[PE]*	[4]	[PE]*
1×6	2.2362	2.2362	1.1257	1.1257
Beam-Theory	2.2504		1.2710	

*[PE]: present element with 24 degrees of freedom.

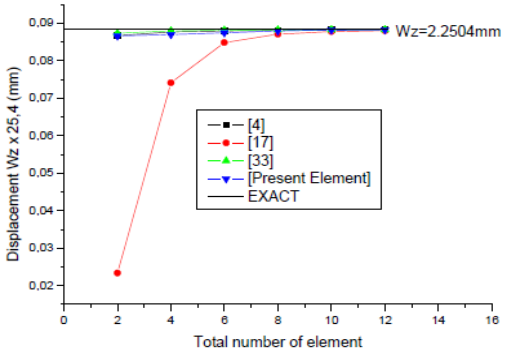

Fig.14
Convergence of displacement Wz for shell-curved beam with static loads.

4 CONCLUSIONS

The present element is a cylindrical shell finite element in a rectangular shape based on strain was developed using deep shell formulations. The element has six degrees of freedom at each corner node, the essential five external degrees of freedom as well as an additional sixth degree of freedom representing the in-plane rotation. The element

is therefore, fully compatible with and can be used in conjunction with arched beam elements having all the essential six degrees of freedom. Using the strain approach for the development of the present element leads to the exact representation of rigid body motions, also leads to higher order polynomial terms without the need for the addition of internal degrees of freedom and has allowed avoiding using finite element of higher order. The performance of the present element has been demonstrated, and the advantage of using the strain approach has been again confirmed. Numerical results obtained using this element agree well with those from other investigations and theoretical results. The present element, while not only successfully solving the pinched cylinder problems for a thin shell is also found when applied to thicker shells, to be at least equal in rapidity of convergence to all other rectangular elements.

Finally, it must be mentioned that the present element is the first strain based cylindrical shell element with in-plane rotation.

APPENDIX A

The way of expressing the deformation in Eq. (4) by [4]:

$$\varepsilon_x = \alpha_7 + \alpha_8\phi$$
$$\varepsilon_\phi = \alpha_9 + \alpha_{10}x - \alpha_{12}x^2/2r - \alpha_{13}x^3/6r - \alpha_{14}x^2\phi/2r - \alpha_{15}x^3\phi/6r$$
$$\varepsilon_{x\phi} = \alpha_{11} + \alpha_8 x/r$$
$$\chi_x = \alpha_{12} + \alpha_{13}x + \alpha_{14}\phi + \alpha_{15}x\phi$$
$$\chi_\phi = \alpha_{16} + \alpha_{17}x + \alpha_{18}\phi + \alpha_{19}x\phi$$
$$\chi_{x\phi} = \alpha_{20} + \alpha_{14}x/r + \alpha_{15}x^2/2r + \alpha_{17}r\phi + \alpha_{19}r\phi^2/2$$

APPENDIX B

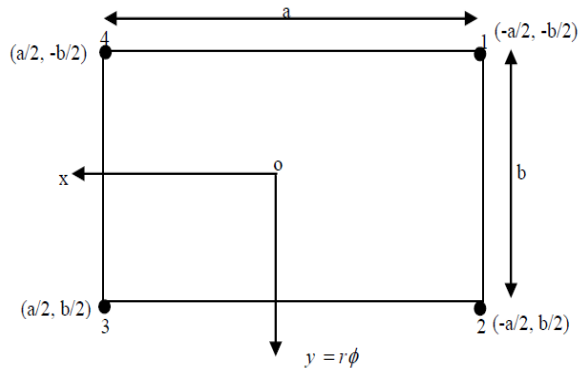

Fig. A2
Rectangular deep shell element with coordinate axes.

From Eq. (8), the 24×24 matrix [A] may be partitioned into the following form:

$$[A] = \left[[A1][A2][A3][A4]\right]^T$$

where the 6×24 matrices $[A_i]$ are given as follow ($i = 1,4$):

$$\begin{bmatrix}
0 & rc_i & 0 & rs_i & 1 & 0 & x_i & \phi_i x_i & 0 & 0 & r\phi_i & 0 & 0 & 0 & 0 \\
s_i & x_i c_i & -c_i & -x_i c_i & 0 & 1 & 0 & 0 & 0 & 0 & 0 & 0 & 0 & 0 & 0 \\
-c_i & x_i c_i & -s_i & -x_i s_i & 0 & 0 & 0 & 0 & r & r x_i & 0 & -\frac{x_i^2}{2} & -\frac{x_i^3}{2} & -\frac{x_i^2\phi_i}{2} & -\frac{x_i^3\phi_i}{6} \\
0 & 0 & 0 & 0 & 0 & 0 & 0 & 0 & 0 & r & 0 & x_i & -\frac{x_i^2}{2} & -x_i\phi_i & -\frac{x_i^2\phi_i}{2} \\
0 & 0 & 0 & 0 & 0 & \frac{1}{r} & 0 & 0 & 0 & 0 & 0 & 0 & 0 & -\frac{x_i^2}{2r} & -\frac{x_i^3}{6r} \\
0 & s_i & 0 & c_i & 0 & 0 & 0 & \frac{x_i}{2r} & 0 & 0 & -\frac{1}{2} & 0 & 0 & 0 & 0
\end{bmatrix}$$

$$\begin{bmatrix}
0 & -\frac{r^2\phi_i^2}{2} & 0 & -\frac{r^2\phi_i - r^2\phi_i^3}{6} & x_i\phi_i & x_i\phi_i^2 & x_i^2\phi_i^3 & r\phi_i & r\phi_i^2 \\
r^2\phi_i^2 & r^2 x_i\phi_i & \frac{r^2\phi_i^2}{2} & \frac{r^2 x_i + r^2 x_i\phi_i^2}{2} & r x_i & 0 & 0 & 0 & 0 \\
-r^2 & -r^2 x_i & r^2\phi_i & r^2 x_i\phi_i & 0 & -r x_i^2 & -2r x_i^3\phi_i & 0 & 0 \\
0 & -r^2 & 0 & r_i^2\phi_i & 0 & -2r_i x_i & -6r x_i^2\phi_i & 0 & 0 \\
-r\phi_i & -r x_i\phi_i & -\frac{r\phi_i^2}{2} - r & -\frac{r x_i\phi_i^2}{2} & -x_i & 0 & -2x_i^3 & 0 & 0 \\
0 & r^2\phi_i & 0 & \frac{r^2\phi_i^2}{2} - r^2 & r & \frac{x_i\phi_i}{r} & \frac{3x_i^2\phi_i^2}{2r} & -x_i & -\phi_i
\end{bmatrix}$$

(x_i, y_i) : are the coordinates of node i $(i = 1,2,3,4)$ as shown in Fig. A2.

where, $\phi_i = \frac{y_i}{r}, c_i = \cos\phi_i, s_i = \sin\phi_i$,

From Eq. (9), the strain matrix $[B]$ for the present element is:

$$[B] = \begin{bmatrix}
0 & 0 & 0 & 0 & 0 & 0 & 1 & \phi & x & \phi & x\phi & 0 \\
0 & 0 & 0 & 0 & 0 & 0 & 0 & 0 & 1 & x & 0 & -\frac{x}{2r} \\
0 & 0 & 0 & 0 & 0 & 0 & 0 & \frac{x}{r} & 0 & 0 & 1 & 0 \\
0 & 0 & 0 & 0 & 0 & 0 & 0 & 0 & 0 & 0 & 0 & 1 \\
0 & 0 & 0 & 0 & 0 & 0 & 0 & 0 & 0 & 0 & 0 & 0 \\
0 & 0 & 0 & 0 & 0 & 0 & 0 & 0 & 0 & 0 & 0 & 0
\end{bmatrix}$$

$$\begin{bmatrix}
0 & 0 & 0 & 0 & 0 & 0 & 0 & 0 & \phi^2 & 2\phi x^3 & 2r\phi & 0 \\
\frac{x^3}{6r} & \frac{x^2\phi}{2r} & \frac{x^3\phi}{6r} & 0 & 0 & 0 & 0 & 0 & -x^2 & -2\phi x^3 & 0 & 0 \\
0 & 0 & 0 & 0 & 0 & 0 & 0 & 0 & \frac{2x\phi}{r} & \frac{3x^2\phi^2}{r} & 2x & 2\phi \\
x & \phi & x\phi & 0 & 0 & 0 & 0 & 0 & 2r & 12x\phi & 0 & 0 \\
0 & 0 & 0 & 1 & x & \phi & x\phi & 0 & 0 & 0 & 0 & 0 \\
0 & \frac{x}{r} & \frac{x^2}{2r} & 0 & r\phi & 0 & \frac{r\phi^2}{2} & 1 & 0 & 6x^2 & 0 & 0
\end{bmatrix}$$

In calculating the element stiffness matrix for the present element, we require the integral (14):

$[K_0] = \int_{-b/2}^{b/2} \int_{-a/2}^{a/2} [B]^T [D][B] dx dy$ is given below:

$[K_0] =$

0	0	0	0	0	0	0	0	0	0	0	0	0	0	0	0	0	0	0	0	0	0	0	0
	0	0	0	0	0	0	0	0	0	0	0	0	0	0	0	0	0	0	0	0	0	0	0
		0	0	0	0	0	0	0	0	0	0	0	0	0	0	0	0	0	0	0	0	0	0
			0	0	0	0	0	0	0	0	0	0	0	0	0	0	0	0	0	0	0	0	0
				0	0	0	0	0	0	0	0	0	0	0	0	0	0	0	0	0	0	0	0
					0	0	0	0	0	0	0	0	0	0	0	0	0	0	0	0	0	0	0
						1	0	2	0	0	3	0	0	0	0	0	0	0	4	0	0	0	0
							5	0	0	0	0	6	0	0	0	0	0	0	0	0	7	0	0
								8	0	0	9	0	0	0	0	0	0	0	10	0	0	0	0
									11	0	0	12	0	0	0	0	0	0	0	0	0	0	0
										13	0	0	0	0	0	0	0	0	0	14	0	0	0
											15	0	0	0	16	0	0	0	17	0	0	0	0
												18	0	0	0	19	0	0	0	0	0	0	0
													20	0	0	0	21	0	0	0	0	22	0
														23	0	0	0	24	25	0	26	0	0
											Symmetrical				27	0	0	0	0	28	0	0	0
																29	0	0	0	0	0	0	0
																	30	0	0	0	0	0	0
																		31	32	0	33	0	0
																			34	0	35	0	0
																				36	0	0	0
																					37	0	0
																						38	0
																							39

where the matrix stiffness element is given below by K_i ($i = 1, \cdots 39$)

K1=D1C1
K2=D2C1
K3=-D2C3/2R
K4=C2D1-C3D2
K5=C2D1+C3D3/R^2
K6=-D2C4/2R
K7=2RC2D1+2C3D3/R^2
K8=C1D1
K9=-D1C3/2R
K-10=C2D2-C3D1
K11=D1C3
K12=-C5D1/R
K13=C1D3
C1=ab
C2=ab^3/12
C3=a^3b/12
L1=4D1C8 + 9D3C/R^2

K14=3D3C4/R
K15=C5D1/4R^2 +K1C1
K16= K2C1
K17= -D2C4/2R +C5D1/2R +2RK1C1
K18=C9D1/36R^2 +K1C3
K19=K2C3
K20=D1C6/4R^2 + K1C2 + K3C3/R^2
K21=K2C2
K22=D2C4
K23=D1C8/36R^2 + K1C4 +K3C5/4R^2
K24=K2C4 + K3C4/4
K25= K3C3/2R
K26=D2C10/3r +D1C8/3r +12rK1C4 + 3K3C5/R
C4=a^3b^3/144
C5=a^5b/180
C6=a^5b^3/960
L2=-36K3C5 +144R^2K1C4

K27=K1C1
K28=2RK2C1
K29=K1C3 + K3R^2C2
K30=K1C2
K31=K1C4 +K3R^2C7/4
K32=RK3C2/2
K33=12RK2C4 + 3RK3C4
K34=K3C1
K35=6K3C3
K36=D1C7
K37=L1+L2+L3
K38=4R^2D1C2+ 4D3C3
K39=4D3C2/R^2
C7=ab^5/80
C8=a^7b^3/5376
C9=a^7b/448
L3=-8D2C+4D1C

APPENDIX C

The derivation of Eq. (3) is described in [3]

Note that: u_0, v_0, w_0 (corresponding to displacements without strains). They become:

$u = u_0(x, \phi), v = v_0(x, \phi), w = w_0(x, \phi)$

$$\varepsilon_x = \frac{\partial u}{\partial x} = 0 \tag{C.1}$$

$$\varepsilon_\phi = \frac{\partial v}{r\partial \varphi} - \frac{w}{r} = 0 \tag{C.2}$$

$$\varepsilon_{x\phi} = \frac{\partial u}{r\partial \phi} + \frac{\partial v}{\partial x} = 0 \tag{C.3}$$

$$\chi_x = \frac{\partial^2 w}{\partial x^2} = 0 \tag{C.4}$$

$$\chi_\phi = \frac{1}{r^2}\left(\frac{\partial v}{\partial \phi} + \frac{\partial^2 w}{\partial \phi^2}\right) = 0 \tag{C.5}$$

$$\chi_{x\phi} = \frac{1}{r}\left(\frac{\partial^2 w}{r\partial x\,\partial \phi} + \frac{\partial v}{r\partial x}\right) = 0 \tag{C.6}$$

We integrate Eqs. (1-6) with all strains equal to zero, after the integration of Eq.(1), we obtain:

$$u = \alpha + g(\phi) \tag{C.7}$$

Using Eq. (2), we obtain:

$$\frac{\partial v}{\partial \phi} = \neg w \tag{C.8}$$

After the integration of Eq. (4), we obtain:

$$\frac{\partial w}{\partial x} = \alpha + A_2(\phi) \Rightarrow w = \alpha x + A_2(\phi)x + A_3(\phi) \tag{C.9}$$

Using (5) and (2), we obtain:

$$\neg w - \frac{\partial^2 w}{\partial \phi^2} = 0 \Rightarrow w = -A_4(x)\cos\phi - A_5(x)\sin\phi \tag{C.10}$$

From the equivalency (9) ≡ (10) and noticing (4), we obtain:

$$\alpha = 0, A_4(x) = \alpha_1 + \alpha_2 x, A_5(x) = \alpha_3 + \alpha_4(x)$$

We substitute α, A_4, A_5 in Eq. (10), we get:

$$w = -(\alpha_1 + \alpha_2 x)\cos\phi - (\alpha_3 + \alpha_4 x)\sin\phi \tag{C.11}$$

From (2) and (11), we obtain:

$$v = -\int w d\phi = -(\alpha_1 + \alpha_2)\sin\phi + (\alpha_3 + \alpha_4)\cos\phi + g_1(x) \tag{C.12}$$

From (6), (11) and (12), we obtain $g_1(x)$:

$$\alpha_2 \sin\phi - \alpha_4 \cos\phi + g_1'(x) - \alpha_2 \sin\phi + \alpha_4 \cos\phi = 0 \Rightarrow g_1'(x) = 0 \Rightarrow g_1(x) = \alpha_6$$

We substitute $g_1(x)$ in (12), we obtain:

$$v = (\alpha_1 + \alpha_2)\sin\phi + (\alpha_3 + \alpha_4)\cos\phi + \alpha_6 \tag{C.13}$$

$$\frac{\partial v}{\partial x} = \alpha_2 \sin\phi - \alpha_4 \cos\phi \tag{C.14}$$

From (3) and (13), we obtain: $u = -r\int \frac{\partial v}{\partial x} d\phi$

$$u = -r\int (\alpha_2 \sin\phi - \alpha_4 \cos\phi) d\phi = r(\alpha_2 \cos\phi + \alpha_4 \sin\phi) + g_2(x) + \alpha_5 \tag{C.15}$$

From the equivalency (7) ≡ (14), we get: $g_2(x) = 0$, then

$$u = r(\alpha_2 \cos\phi + \alpha_4 \sin\phi) + \alpha_5 \tag{C.16}$$

REFERENCES

[1] Belarbi M.T. , Bourezane M., 2005, On improved sabir triangular element with drilling rotation, *Revue Européenne de Genie Civil* **9**: 1151-1175.

[2] Belarbi M.T., 2000, *Developpement de Nouvel Element Fini Base Sur le Modele en Deformation*, Application Lineaire et Non Lineaire, Phd Thesis, University of Constantine, Algeria.

[3] Bourezane M., 2006, *Utililisation of the Strain Model in the Analysis of the Structures*, Phd Thesis, University of Biskra, Algeria.

[4] Ashwell D.G., Sabir A.B., 1972, A new cylindrical shell finite element based on simple independent strain functions, *International Journal of Mechanical Sciences* **14**: 171-183.

[5] Lindberg G.M., Olson M.D., Cowper G.R., 1969, *New Development in the Finite Element Analysis of Shells*, Structures and Materials Laboratory National Aeronautical Establishment, National Research Council of Canada.

[6] Yang T.Y., 1973, High order rectangular shallow shell finite element, *Journal of Engineering Mechanics* **99**: 157-181.

[7] Dawe D.J., 1975, High order triangular finite element for shell analysis, *International Journal of Solids Structures* **11**: 1097-1110.

[8] Hrennlkoff A., Tezcan S.S, 1968, Analysis of cylindrical shells by the finite element method, *Sympoium on Problems of Interdependence of Design and Construction of Large Span Shells*, Lenigrad.

[9] Zienkiewicz O.C., Cheng Y.K., 1967, *The Finite Element in Structural and Continuum Mechanics*, Mc Graw Hill, Book Co, London.

[10] Clough R.W., Johnson R.G., 1968, A finite element approximation for the analysis of thin shells, *International Journal for Solids and Structures* **4**: 43-60.

[11] Carr A.J., 1967, *A Refined Finite Element Analysis of Thin Shell Structures Including Dynamic Loadings*, Phd Thesis, University of California, Berekely.

[12] Bogner F.K., Fox R.L., Schmit L.A., 1967, A cylindrical shell discrete element, *AIAA Journal* **5**: 745-750.

[13] Cantin G., Clouth R.W., 1968, A curved cylindrical shell Finite Element, *AIAA Journal* **6**: 1057-1062.

[14] Olson M.D., Lindberg G.M., 1968, Vibration analysis of cantilevered curved plates usisng a new cylindrical shell finite element, *Proceedings of the Second Conference on Matrix Methods in Structural Mechanics* ,Wright- Patterson AFB, Ohio.

[15] Ashwell D.G., Sabir A.B., 1971, Limitations of certain curved finite elements when applied to arches, *International Journal of Mechanical Sciences* **13**: 133-139.

[16] Ashwell D.G., Sabir A.B., Roberts T.M., 1971, Further studies in the application of curved elements to circular arches, *International Journal of Mechanical Sciences* **13**(6): 507-517.

[17] Sabir A.B., Lock A.C., 1972, A curved cylindrical shell finite element, *International Journal of Mechanical Sciences* **14**(2): 125-135.

[18] Sabir A.B., Sfendji A., 1995, Triangular and rectangular plane elasticity finite elements, *Thin Walled Structures* **21**(3): 225-232.
[19] Sabir A.B., Moussa A.I. , 1997, Analysis of fluted conical shell roofs using the finite element method, *Computer and Structures* **64** (1-4): 239-251.
[20] Sabir A.B., Salhi H.Y., 1986, A strain based finite element for general plane elasticity problems in polar coordinates, *Research Mechanica* **19**: 1-6.
[21] Sabir A.B., 1983, Strain based finite elements for the analysis of cylinders with holes and normally intersecting cylinders, *Nuclear Engineering and Design North-Holland* **76**: 111-120.
[22] Sabir A.B., Ashwell D.G., 1969, A stiffness matrix for shallow shell finite elements, *International Journal of Mechanical Science* **11**: 269-279.
[23] Sabir A.B., Ramadani F., 1985, A shallow shell finite element for general shell analysis, *Proceedings of the 2nd International Conference on Variational Methods in Engineering*.
[24] Sabir A.B., 1983, A new class of finite elements for plane elasticity problems, *CAFEM 7th, International Conference on Structural Mechanics in Reactor Technology*,Chicago.
[25] Trinh V.D., Abed-Meriam F., Comberscure A., 2011, Assumed strain solid- shell formulation "SHB6'' for the six node prismatic, *Journal of Mechanical Science and Technology* **25**(9): 2345-2364.
[26] Mousa A.I., EINaggar M.H., 2007, Shallow spherical shell rectangular finite element for analysis of cross shaped shell roof, *Electronic Journal of Structural Engineering* **7**: 41-51.
[27] Rebiai C., Belounar L., 2013, A new strain based rectangular finite element with drilling rotation for linear and nonlinear analysis, *Archives of Civil and Mechanical Engineering* **13**: 72-81.
[28] Djoudi M.S., Bahi H., 2003, A shallow shell finite element for the linear and nonlinear analysis of cylindrical shells, *Engineering Structures* **25**(6):769-778.
[29] Sabir A.B., Djoudi M.S., 1995, Shallow shell finite element for the large deflection geometrically nonlinear analysis of shells and plates, *Thin Wall Structures* **21**: 253-267.
[30] Timoshenko S., Woinoisky-Kreiger S., 1959, *Theory of Plates and Shells*, Mc Graw-Hill, New York.
[31] Charchafchi T.A., Sabir A.B., 1982, *Curved Rectangular and General Quadrilateral Shell Element for Cylindrical Shells*,The Mathematics of Finite Element and Applications , Whiteman Academic Press.
[32] Cantin G., 1970, Rigid body motions in curved finite elements, *AIAA Journal* **8**: 1252-1255.
[33] Bull J.W., 1984, The strain approach to the development of thin cylindrical shell finite element, *Computer and Structures* **2**(3): 195-205.
[34] Batoz J.L., Dhatt G., 1992, *Modélisation des Structures par Eléments Finis*, Coques, Eds Hermès, Paris.
[35] MacNeal R. H., Harder R. L., 1985, A proposed standard set of problems to test finite element accuracy, *Finite Elements in Analysis and Design* **1**: 3-20.